ACS APPLIED MATERIALS & INTERFACES

Research Article

www.acsami.org

Facile Synthesis of Molecularly Imprinted Graphene Quantum Dots for the Determination of Dopamine with Affinity-Adjustable

Xi Zhou, Anqi Wang, Chenfei Yu, Shishan Wu,* and Jian Shen*

School of Chemistry and Chemical Engineering, Nanjing University, Nanjing 210093, China

Supporting Information

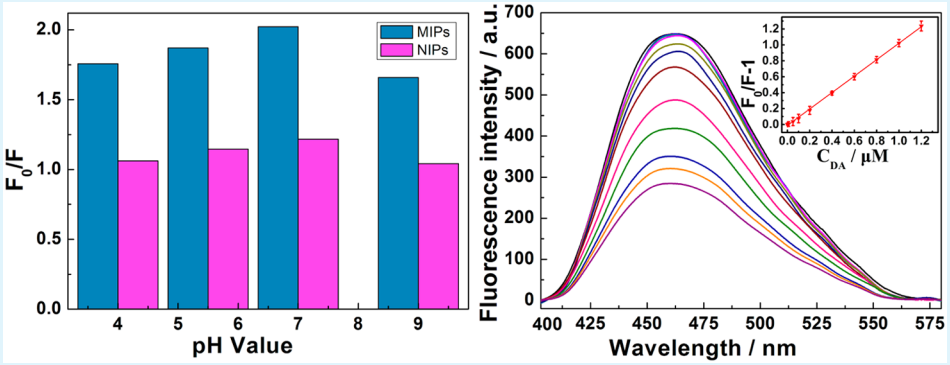

ABSTRACT: A facilely prepared fluorescence sensor was developed for dopamine (DA) determination based on polyindole/graphene quantum dots molecularly imprinted polymers (PIn/GQDs@MIPs). The proposed sensor exhibits a high sensitivity with a linear range of 5×10^{-10} to 1.2×10^{-6} M and the limit of detection as low as 1×10^{-10} M in the determination of DA, which is probably due to the tailor-made imprinted cavities for binding DA thought hydrogen bonds between amine groups of DA and oxygen-containing groups of the novel composite. Furthermore, the prepared sensor can rebind DA in dual-type: a low affinity type (noncovalent interaction is off) and a high affinity type (noncovalent interaction is on), and the rebinding interaction can be adjusted by tuning the pH, which shows a unique potential for adjusting the binding interaction while keeping the specificity, allowing for wider applications.

KEYWORDS: *molecularly imprinted polymer, graphene quantum dots, fluorescence, polyindole, dopamine, affinity-adjustable*

INTRODUCTION

Dopamine (DA), one of the crucial neurotransmitters in the human central nervous system, has aroused considerable interest because of its potential therapeutics for neurological and psychiatric disorders.[1,2] Lewis et al. proved the role as neuroprotective agents of DA agonists in Parkinson's disease.[3] In addition, some other movement disorders, including Ekbom's restless syndrome, are also correlated to the abnormal concentration of DA.[4,5] Therefore, a precise and sensitive way of DA detection in the diagnostics of relevant mental diseases is extremely needed. Although various methods such as electrochemistry,[6,7] ultraviolet−visible spectrophotometry,[8] and enzymatic method,[9] have been developed to solve these issues, the determination of DA remains challenging. Particularly, universal, efficient and facile approaches for DA detection are still rather limited.[10,11] Compared with the chemical and biological approaches, fluorescence spectroscopy for DA analysis has attracted considerable attention because of its excellent performance, including time saving, simple operation, fast response, cost effectiveness, good stability, and reproducibility.

In the past decades, semiconductor quantum dots (SQDs) have received extensive interest for their unique optical performance.[12,13] However, the intrinsic defects of those SQDs such as heavy metals potential toxicity and environmental hazards, which limit their widespread application.[14] Therefore, the development of eco-friendly alternatives is highly desirable. Recently, graphene quantum dots (GQDs), as a metal-free quantum dots system, show strong potential for replacing traditional SQDs.[15] Due to quantum confinement and edge effects, GQDs possess fascinating features such as high photostability and fluorescence activity.[16,17] Furthermore, GQDs constitute a superior class of devices for bioimaging because of their attractive properties, such as remarkable biocompatibility, low cytotoxicity and eco-friendliness.[18,19] However, few GQD-based fluorescence sensors have been reported, which may be due to the difficulty in searching for GQDs that can both give sensitive signal response and selectively identify a target.[20]

Molecular imprinting technique is a system of design and construction of tailor-made sensors with specific recognition and three-dimensional cavities for the target molecules.[21] In

Received: November 10, 2014
Accepted: January 5, 2015
Published: January 20, 2015

DOI: 10.1021/am5078478
ACS Appl. Mater. Interfaces 2015, 7, 11741−11747

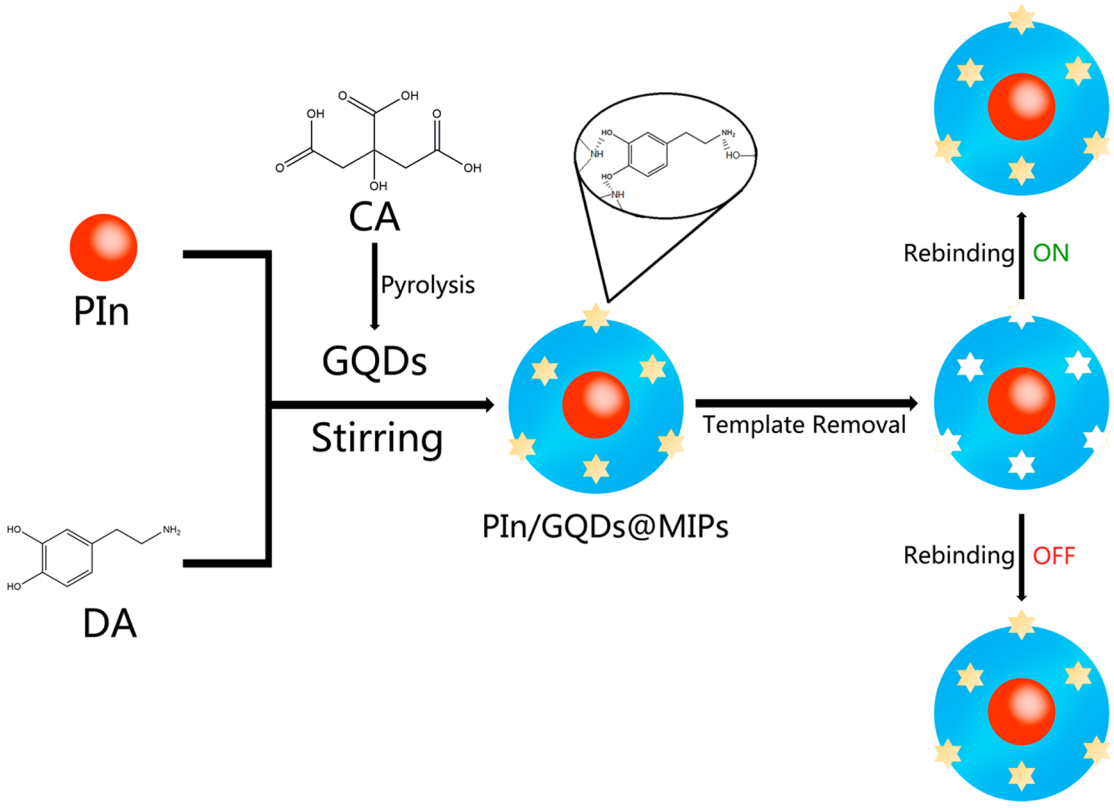

Figure 1. Illustration of the preparation of PIn/GQDs@MIPs.

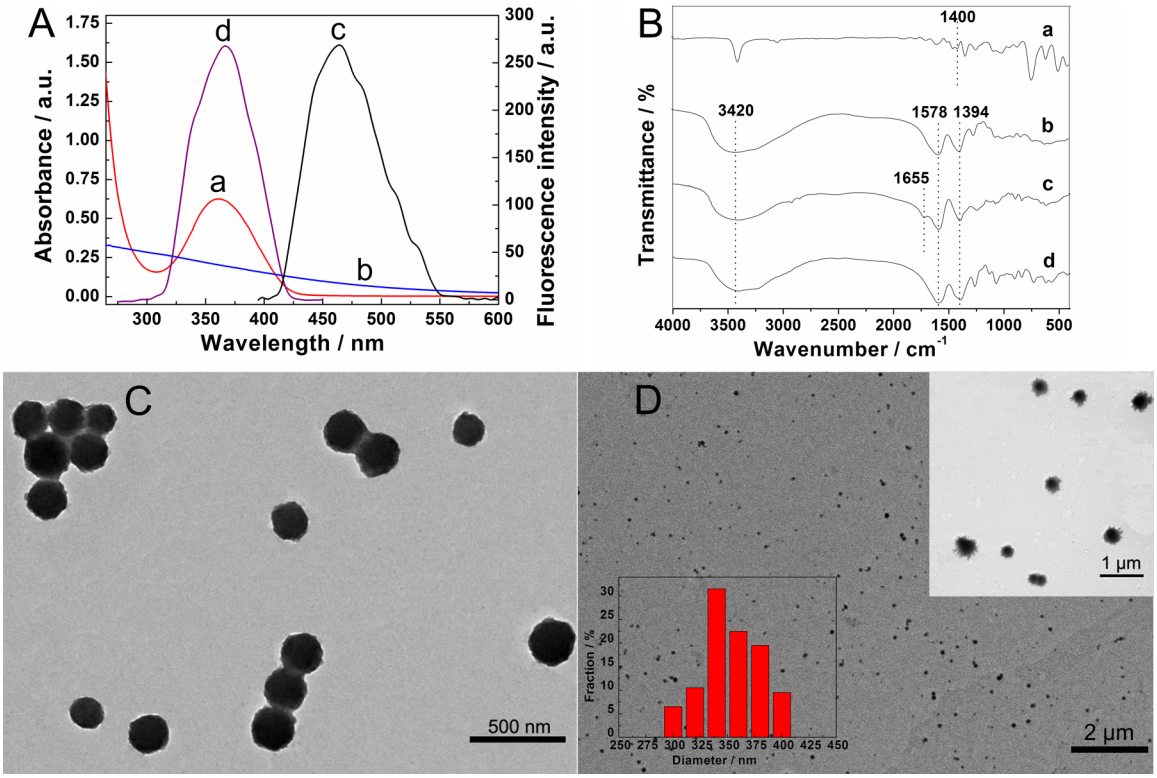

Figure 2. (A) UV−vis absorption spectra of (a) PIn/GQDs@MIPs, (b) PIn. (c) Emission and (d) excitation fluorescence spectra of PIn/GQDs@MIPs. (B) FT-IR spectra of (a) PIn, (b) PIn/GQDs@NIPs, PIn/GQDs@MIPs (c) before and (d) after template molecules extraction. The TEM images of (C) PIn and (D) PIn/GQDs@MIPs (upper right inset: the enlarged TEM image of PIn/GQDs@MIPs, bottom left inset: the corresponding size distribution of PIn/GQDs@MIPs).

DOI: 10.1021/am5078478
ACS Appl. Mater. Interfaces 2015, 7, 11741−11747

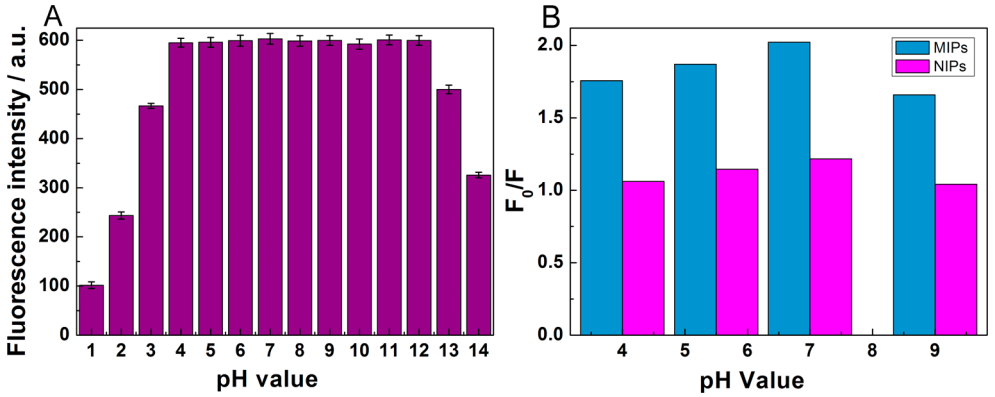

Figure 3. (A) Fluorescence intensity of PIn/GQDs@MIPs at different pH values. (B) Fluorescence responses of PIn/GQDs@MIPs and PIn/GQDs@NIPs in the absence and presence of 1 μM DA at different pH values. F_0 and F are the fluorescence intensity in the absence and presence of DA, respectively.

contrast to other functionalized materials, molecular imprinting polymers (MIPs) show notable features such as good stability, strong affinity, easy fabrication, and low cost, and thus have been proved as one of the most competitive tools in the field of biomolecules recognition.[10] Recently, molecular imprinting and fluorescent sensor techniques have been incorporated to construct fluorescent sensors based on MIPs, which have been reported and demonstrated the achievement of recognition and detection for DA. Xue et al. constructed a composite of gold nanoparticles doped molecularly imprinted polymers for DA detection.[22] Mao et al. prepared a fluorescent sensor for DA based on silica molecular imprinted nanospheres.[23] Recently, there has been increasing interest in polyindole (PIn), which possesses the attributes of both poly(para-phenylene) and polypyrrole together, including slow degradation rate, good thermal stability, and high redox activity.[24] Moreover, the amine group on the heterocycle may lead to enhancement of biomolecular sensing.[25]

The present study reports an efficient and facile strategy for DA detection by using a novel composite of PIn/GQDs@MIPs. PIn microspheres were first synthesized from indole by the initiation of a $FeCl_2-H_2O_2$ mixture. PIn/GQDs@MIPs were then prepared by pyrolysis citric acid (CA) and adding it into PIn-DA system under vigorous stirring (Figure 1). After that, the template DA was removed by disrupting the noncovalent binding in an acidic condition, leaving three-dimensional cavities that were complementary to the molecular shape of the template. The nitrogen heteroatoms and oxygen-containing groups incorporated into the composite enable it to attract DA molecules effectively by hydrogen bonds.[26] Furthermore, different from MIPs synthesized by the other approaches, MIPs prepared by this process can rebind the DA molecules in dual types: at a high pH that allows a firm interaction, the rebinding is due to the shape matching and noncovalent binding (high affinity binding type), whereas at a low pH that disrupts the noncovalent binding, the rebinding is principally due to shape matching (low affinity binding type). The affinity degree of MIPs toward DA can be tuned by controlling the binding pH. To the best of our knowledge, such a dual-type binding mechanism in DA analysis has never been found in the literature.

RESULTS AND DISCUSSION

To investigate the optical properties of composites, we carried out fluorescence and UV−vis absorption spectroscopy (Figure 2A). The prepared MIPs present a symmetric fluorescence emission peak at 465 nm when excited at 366 nm. At the same time, Fourier transform infrared (FT-IR) spectral (Figure 2B) reveal a characteristic peak at about 1400 cm^{-1} for the C−N bonding vibration of PIn, whereas in the MIPs and NIPs, this peak transfers from 1400 to 1394 cm^{-1} because of protonation from the carboxylic acid functional group of GQDs. And the broad adsorption band between 3000 and 3700 cm^{-1} can be attributed to O−H stretching vibration of hydroxyl groups linked to MIPs and NIPs composites.[27] Besides, both MIPs and NIPs have a characteristic peak at about 1578 cm^{-1} corresponding to the bonding vibration of −COOH.[28] The characteristic peak of MIPs (Figure 2Bc) at 1655 cm^{-1} can be ascribed to the exclusive stretching bands of $-NH_3^+$ in DA molecule. After solvent elution, this characteristic peak disappeared in Figure 2Bd, which suggest that the DA molecules have been washed out during the extraction process.[29] Moreover, transmission electron microscopy (TEM) images (Figure 2C, D and Figure S1B in the Supporting Information) display a typically smooth surface microsphere structure of PIn and a distinct core/shell morphology of MIPs and NIPs, in both of which GQDs are present at the periphery of PIn microsphere. This probably be due to $\pi-\pi$ interaction between PIn and the sp^2 π clouds of GQDs.[27] NIPs shows the similar appearances with MIPs Furthermore, X-ray photoelectron spectroscopy (XPS) was employed to verify the presence of oxygen-containing group. From Figure S1A in the Supporting Information, we can find that the peaks of N 1s and O 1s in the pristine PIn are obviously observed, which confirms the presence of oxygen-containing groups. Besides, particle size statistics (the inset of Figure 2D) show that the diameters of MIPs are mainly distributed in the range of 295−400 nm with a mean size of 353 ± 12 nm.

To reveal the effect of pH valve on fluorescence intensity, we studied the fluorescence responses of MIPs at different pH. As showed in Figure 3A, the fluorescence intensity of MIPs is obviously pH dependent and relatively low in strong acidic and alkali conditions. To further investigate the interactions between DA and composites, rebinding experiments for MIPs and NIPs at different pH valve were carried out. The results are presented in Figure 3B, in which the fluorescence response of MIPs toward DA is much higher than that of NIPs under all the conditions. As a comparison, for the NIPs, no obvious response is recorded at the same pH value. These results indicate that the

DOI: 10.1021/am5078478
ACS Appl. Mater. Interfaces 2015, 7, 11741−11747

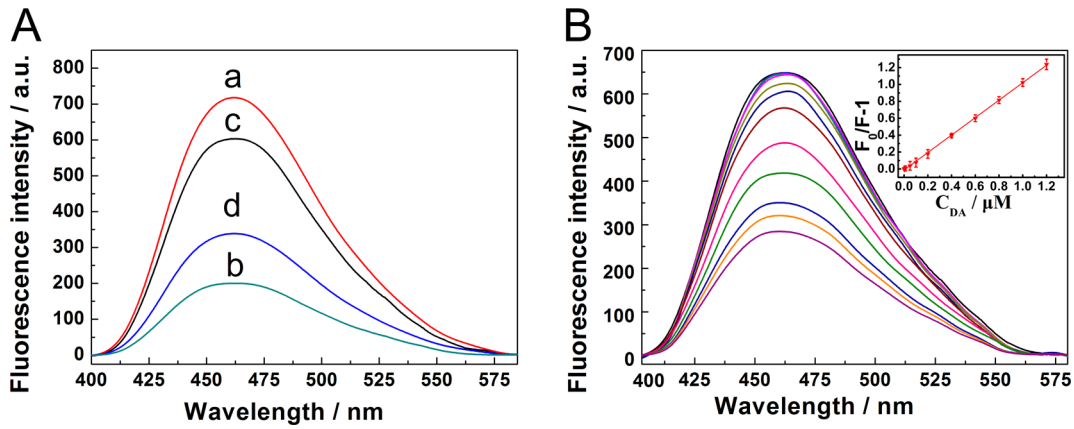

Figure 4. (A) Fluorescence emission spectra of (a) PIn/GQDs@NIPs, PIn/GQDs@MIPs (b) before and (c) after template molecules extraction, (d) PIn/GQDs@MIPs with addition of 1 μM DA. (B) Fluorescence emission spectra of PIn/GQDs@MIPs with addition of the indicated concentrations of DA, which were 0, 0.0005, 0.001, 0.005, 0.01, 0.05, 0.1, 0.2, 0.4, 0.6, 0.8, 1.0, 1.2 μM (from top to bottom), respectively (inset: the calibration curve of DA obtained with PIn/GQDs@MIPs).

specific affinity of the MIPs toward the template is due to the well-fabricated imprinting cavities rather than nonspecific adsorption. Compared with the NIPs, the MIPs have more binding sites suitable for DA because of an efficient imprinting effect. As Figure 3B revealed, even at pH 4.0, at which noncovalent binding is inactivated,[10] the MIPs still exhibit a strong enough interaction with DA. This confirms the presence of the low affinity binding type. Such an affinity is mainly due to the shape matching between the template molecule and the imprinted cavities. At pH 5.5, the binding condition is moderate between the high and low affinity type. At pH 9.0, the electrostatic repulsion between the electronegative parts of proposed sensor and DA (pK_a = 8.75) anions slightly offsets the noncovalent binding, which could repel the rebinding of DA. The high affinity binding type at pH 7.0 can be rationalized not only by the tailor-made imprinted cavities but also the stronger noncovalent binding. It is clearly that the rebinding interaction could be tuned by adjusting the surrounding pH, which shows a unique potential for adjusting the binding interaction while holding the specificity, allowing for wider applications.

The prepared fluorescent MIPs material can be further applied to DA detection. As shown in Figure 4A, after DA extraction, the fluorescence of MIPs (curve c) nearly reaches that of NIPs (curve a). Besides, the fluorescence intensity of MIPs without templates is quenched a lot when interact with target molecules (curve d), and a photoinduced electron transfer (PET) between DA and MIPs is suggested as the mechanism of fluorescence quenching. When the hydroxyl and amine groups of DA interact with the oxygen-containing groups of MIPs, the lone pair of electrons of the oxygen-containing groups is available for photoinduced electron transfer or intramolecular charge transfer, leading to a decrease in the fluorescence.[28]

We find that the fluorescence quenching effect in this system can be quantified by a Stern−Volmer equation

$$F_0/F = 1 + K_{sv}C_{DA}$$

where F_0 and F are the fluorescence intensities in the absence and presence of DA, respectively, K_{sv} is the quenching constant of DA, and C_{DA} is the concentration of DA.[30]

Figure 4B shows the fluorescence responses of MIPs at different concentrations of DA. The fluorescence quenching efficiency (F_0/F −1) increased with a linear relationship between the fluorescence quenching efficiency and the concentrations of DA in the range of 0.5−1200 nM (R = 0.9993). The limit of detection (LOD) for DA is 0.1 nM based on the situation that the signal-to-noise ratio is 3 (S/N = 3). Furthermore, the slope of the calibration plot of MIPs toward DA is 5 times higher than that of NIPs (see Figure S2 in the Supporting Information). It is worthwhile noticing that the sensitivity of the prepared MIPs toward DA is much higher than that of other published quantum dots-based and molecular imprinting polymers modified materials (see Table S1 in the Supporting Information). These phenomena indicate low detection limit and high sensitivity of the prepared MIPs sensor.

To assess the reliability and applicability of PIn/GQDs@MIPs fluorescent biosensor, which was employed for analysis DA in human serum and urine samples, standard addition method was used to obtain a quantitative recovery ranged from 93.81 to 108.08%, as shown in Table 1. The detection result indicates the good accuracy and the great potential applicability of prepared sensor for DA analysis in real samples.

Table 1. Determinations of DA in Human Serum and Urine Samples

sample	spike (nM)	found (nM)	recovery (%)	RSD (n = 3, %)
serum	50.00	52.65	105.30	3.38
	100.00	93.81	93.81	2.16
	200.00	192.30	96.15	3.93
	500.00	516.15	103.23	2.72
	1000.00	1080.80	108.08	4.27
urine	50.00	47.37	94.73	1.91
	100.00	96.29	96.29	3.72
	200.00	211.34	105.67	4.33
	500.00	535.45	107.09	2.19
	1000.00	987.80	98.78	2.78

To study the reproducibility of the proposed method, we used five prepared sensors to measure 1 μM DA with fluorescence, which shows similar responses and the relative standard deviation (RSD) of 4.5%. These results indicate good reproducibility of the proposed sensor. Meanwhile, the stability of prepared sensor was investigated through measuring

DOI: 10.1021/am5078478
ACS Appl. Mater. Interfaces 2015, 7, 11741−11747

fluorescence intensity of the sensor, which lost less than 6.8% of the initial intensity after storage for 2 weeks. This demonstrates that the prepared sensor possesses good stability.

The selectivity of MIPs sensor was investigated by comparing the fluorescence response with respect to functional and structural interfering analogues such as 3,4-dihydroxyphenylacetic acid (DOPAC), norepinephrine (NE), 5-Hydroxyindole acetic acid (5-HIAA) and Epinephrine (EP), and some coexistent interferents such as uric acid (UA) and ascorbic acid (AA). A significant selective quenching effect by DA over other interferents could be observed in this assay (Figure 5, green columns), which suggest a better adsorption and binding capacity for the target molecules. Moreover, in order to further research the specificity of the proposed sensor, the comparison of fluorescence responses between MIPs and NIPs for DA and those interferents was carried out. From Figure 5, we can find that the five analogues nearly quenched the fluorescence of NIPs with the same efficiency, which were lower than those of MIPs. These results further confirm the high specific recognition of MIPs for the templates is mainly due to the specific binding between MIPs and DA as well as the tailor-made imprinted cavities with DA, showing great promise for DA detection in real samples.

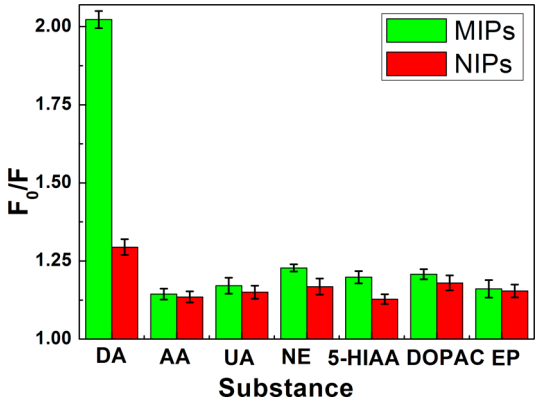

Figure 5. Selective adsorption of DA and the other five biological molecules (AA, UA, NE, 5-HIAA, DOPAC, EP) by PIn/GQDs@MIPs and PIn/GQDs@NIPs. F_0 and F are the fluorescence intensity of PIn/GQDs@MIPs in the absence and presence of biological molecules, respectively.

To further investigate the capacity of resisting disturbance of MIPs sensor for DA in the presence of interferents, we measured the fluorescence response using standard titrations in the presence of DA, with interferents such as AA, UA, NE, 5-HIAA, DOPAC, EP. As shown in Figure S3A in the Supporting Information, the fluorescence quenching efficiencies of sensors are quite close to each other, which confirms selective discrimination of DA against interferents. Moreover, Figure S3B in the Supporting Information shows the fluorescence response of MIPs sensor for DA in a concentration range of 5×10^{-4} to 1 μM with a linearity correlation coefficient of 0.990, in the presence of above six interferents. Further determination results reveal that the concentration ratio of 1/1000, 1/1000, 1/800, 1/800, 1/800, and 1/800 for AA, UA, NE, 5-HIAA, DOPAC, and EP could not disturb the determination of DA, which demonstrates that the MIPs can serve as highly selective fluorescent sensor for DA analysis.

CONCLUSIONS

In summary, a new sensing approach based on molecularly imprinted graphene quantum dots, inducing a PET process to analyze DA effectively, has been successfully developed, and a unique affinity-adjustable dual-type binding mechanism has been demonstrated. It took advantages of fluorescence spectroscopy method, graphene quantum dots and molecular imprinting technique, which can both give sensitive signal response and selectively identify DA molecule, and proved to be simple in design and economic in operation, showing distinct superiorities over existing strategies, such as tunable binding interaction, fast response, and high sensitivity. The dual-type provided a unique possibility to adjust the binding interaction while keeping the specificity. Furthermore, this new understanding of the binding mechanism in molecular imprinting can promote not only the development of new MIPs but also the design of other biological sensing materials, which will be beneficial for biological and environmental applications.

EXPERIMENTAL SECTION

Fabrications of the PIn Nanospheres. PIn was initiated with the addition of 2.5 mL of H_2O_2 to the indole/$FeCl_2$/H_2O (0.1 g/0.05 g/97.5 mL) mixture and lasted for 6 h. After that, centrifugation was used for collecting the product, which had been washed with water several times to remove reaction byproducts and unused reactants. Finally, the prepared PIn was dried in vacuum at 35 °C.

Fabrications of the PIn/GQDs@MIPs and PIn/GQDs@NIPs Sensor. The synthesis of PIn/GQDs@MIPs was initiated by hydrothermal treatment of citric acid (CA) into PIn/DA/H_2O system. One gram of CA monohydrate was heated to 200 °C in a 5 mL beaker by a heating mantle, until the CA changed to an orange liquid. Then, the liquid was dissolved into the PIn/DA/H_2O (0.1 g/0.1 g/50 mL) mixture and further neutralized with NaOH, with vigorous stirring for 3 h. The resulting product was concentrated by centrifugation, and eluted with deionized water and ethanol-acetic acid (49:1, v/v) to remove DA. Fabrication processes of nonimprinted polymers (PIn/GQDs@NIPs) were as same as the approach mentioned above but without the addition of DA.

Fluorescence Measurements. In a typical assay, PIn/GQDs@MIPs solution (200 μL, pH 7.0), 0.1 mol/L PBS buffer (pH 7.0, 1 mL), and different amounts of DA or other interferents (AA, UA, NE, DOPAC, 5-HIAA and EP) were added into a 5 mL cuvette. Then the solution was diluted to the mark with deionized water and incubated at room temperature for 30 min. Fluorescence measurement was carried out under excitation at 366 nm. The fluorescence spectra were recorded from 370 to 700 nm, and the slit widths of emission and excitation were both 4 nm.

Instruments and Measurements. Fourier transform infrared (FT-IR) spectra were taken from KBr pellets of the samples on a Nicolet NEXUS870 spectrometer. UV−vis spectra were carried out on a Lambda 35 PerkinElmer spectrometer. UV−vis spectra samples were prepared by dilution specimen solution into a 1 cm quartz cell and incubating at room temperature for 30 min. Fluorescence measurements were performed on an LS SS PerkinElmer spectrometer. X-ray photoelectron spectroscopy (XPS) measurements were performed on a PHI 5000 VersaProbe. All transmission electron microscopy (TEM) images were obtained by a JEM 2100 high-resolution TEM. TEM samples were prepared by drop coating the suspension onto a carbon coated copper grid with a 400 μm diameter hole.

ASSOCIATED CONTENT

Supporting Information

XPS spectra of PIn, TEM images of NIPs, FT-IR spectra of DA and GQDs, fluorescence responses of PIn/GQDs@NIPs with increasing DA concentration, resisting disturbance experiments,

DOI: 10.1021/am5078478
ACS Appl. Mater. Interfaces 2015, 7, 11741−11747

and comparison of this work with some established methods using MIPs to detect dopamine. The Supporting Information is available free of charge on the ACS Publications website at DOI: 10.1021/am5078478.

AUTHOR INFORMATION

Corresponding Authors

*E-mail: shishanwu@nju.edu.cn.

*E-mail: shenj57@nju.edu.cn.

Author Contributions

The manuscript was written through contributions of all authors. All authors have given approval to the final version of the manuscript.

Notes

The authors declare no competing financial interest.

ACKNOWLEDGMENTS

This work was supported by the National Natural Science Foundation of China (51272100, and 51273073).

REFERENCES

(1) Zhang, A.; Neumeyer, J. L.; Baldessarini, R. J. Recent Progress in Development of Dopamine Receptor Subtype-Selective Agents: Potential Therapeutics for Neurological and Psychiatric Disorders. *Chem. Rev.* **2007**, *107*, 274−302.

(2) Ho, C. C.; Ding, S. J. Dopamine-Induced Silica−Polydopamine Hybrids with Controllable Morphology. *Chem. Commun.* **2014**, *50*, 3602−3605.

(3) Lewis, M. M.; Huang, X.; Nichols, D. E.; Mailman, R. B. D1 and Functionally Selective Dopamine Agonists as Neuroprotective Agents in Parkinson's Disease. *CNS Neurol. Disord.: Drug Targets* **2006**, *5*, 345−353.

(4) Feng, J. J.; Guo, H.; Li, Y. F.; Wang, Y. H.; Chen, W. Y.; Wang, A. J. Single Molecular Functionalized Gold Nanoparticles for Hydrogen-Bonding Recognition and Colorimetric Detection of Dopamine with High Sensitivity and Selectivity. *ACS Appl. Mater. Interfaces* **2013**, *5*, 1226−1231.

(5) Dong, X. C.; Wang, X. W.; Wang, L. H.; Song, H.; Zhang, H.; Huang, W.; Peng, C. 3D Graphene Foam as a Monolithic and Macroporous Carbon Electrode for Electrochemical Sensing. *ACS Appl. Mater. Interfaces* **2012**, *4*, 3129−3133.

(6) Ma, Y.; Zhao, M. G.; Cai, B.; Wang, W.; Ye, Z. Z.; Huang, J. Y. 3D Graphene Network@WO3 Nanowire Composites: a Multifunctional Colorimetric and Electrochemical Biosensing Platform. *Chem. Commun.* **2014**, *50*, 11135−11138.

(7) Hsu, M. S.; Chen, Y. L.; Lee, C. Y.; Chiu, H. T. Gold Nanostructures on Flexible Substrates as Electrochemical Dopamine Sensors. *ACS Appl. Mater. Interfaces* **2012**, *4*, 5570−5575.

(8) Yu, T.; Liu, Y. H.; Ren, J. S.; Qu, X. G. A Dual Fluorometric and Colorimetric Sensor for Dopamine based on BSA-stabilized Au Nanoclusters. *Biosens. Bioelectron.* **2013**, *42*, 41−46.

(9) Fritzen-Garcia, M. B.; Monteiroa, F. F.; Cristofolini, T.; Zanetti-Ramos, B. G.; Soldi, V.; Pasa, A. A.; Creczynski-Pasa, T. B. MEMS-Based Multi-inlet/outlet Preconcentrator Coated by Inkjet Printing of Polymer Adsorbents. *Sens. Actuators, B* **2013**, *182*, 264−272.

(10) Wang, S. S.; Ye, Z.; Bie, Z. J.; Liu, Z. Affinity-Tunable Specific Recognition of Glycoproteins via Boronate Affinity-based Controllable Oriented Surface Imprinting. *Chem. Sci.* **2014**, *5*, 1135−1140.

(11) Huang, Y. P.; Miao, Y. E.; Ji, S. S.; Tjiu, W. W.; Liu, T. X. Electrospun Carbon Nanofibers Decorated with Ag−Pt Bimetallic Nanoparticles for Selective Detection of Dopamine. *ACS Appl. Mater. Interfaces* **2014**, *6*, 12449−12456.

(12) Silva, A. C. A.; Silva, M. J. B.; Cordero da Luz, F. A.; Silva, D. P.; Vieira de Deus, S. L.; Dantas, N. O. Controlling the Cytotoxicity of CdSe Magic-Sized Quantum Dots as a Function of Surface Defect Density. *Nano Lett.* **2014**, *14*, 5452−5457.

(13) Liu, S. F.; Zhang, X.; Yu, Y. M.; Zou, G. Z. A Monochromatic Electrochemiluminescence Sensing Strategy for Dopamine with Dual-Stabilizers-Capped CdSe Quantum Dots as Emitters. *Anal. Chem.* **2014**, *86*, 2784−2788.

(14) Liu, Y.; Wu, P. Y. Graphene Quantum Dot Hybrids as Efficient Metal-Free Electrocatalyst for the Oxygen Reduction Reaction. *ACS Appl. Mater. Interfaces* **2013**, *5*, 3362−3369.

(15) Moon, J. H.; An, J. H.; Sim, U.; Cho, S. P.; Kang, J. H.; Chung, C.; Seo, J. H.; Lee, J. H.; Nam, K. T.; Hong, B. H. One-Step Synthesis of N-Doped Graphene Quantum Sheets from Monolayer Graphene by Nitrogen Plasma. *Adv. Mater.* **2014**, *26*, 3501−3505.

(16) Dong, Y. Q.; Pang, H. C.; Yang, H. B.; Guo, C. X.; Shao, J. W.; Chi, Y. W.; Li, C. M.; Yu, T. Carbon-Based Dots Co-Doped with Nitrogen and Sulfur for High Quantum Yield and Excitation-Independent Emission. *Angew. Chem., Int. Ed.* **2013**, *52*, 7800−7804.

(17) Yu, X. J.; Liu, J. J.; Yu, Y. C.; Zuo, S. L.; Li, B. S. Preparation and Visible Light Photocatalytic Activity of Carbon Quantum Dots/TiO_2 Nanosheet Composites. *Carbon* **2014**, *68*, 718−724.

(18) Ogaidi, I. A.; Gou, H. L.; Aguilar, Z. P.; Guo, S. W.; Melconian, A. K.; Al-kazaz, A. K. A.; Meng, F. K.; Wu, N. Q. Detection of the Ovarian Cancer Biomarker CA-125 using Chemiluminescence Resonance Energy Transfer to Graphene Quantum Dots. *Chem. Commun.* **2014**, *50*, 1344−1346.

(19) Russo, P.; Hu, A. M.; Compagnini, G.; Duley, W. W.; Zhou, N. Y. Femtosecond Laser Ablation of Highly Oriented Pyrolytic Graphite: a Green Route for Large-Scale Production of Porous Graphene and Graphene Quantum Dots. *Nanoscale* **2014**, *6*, 2381−2389.

(20) Dong, Y. Q.; Wang, R. X.; Li, H.; Shao, J. W.; Chi, Y. W.; Lin, X. M.; Chen, G. N. Polyamine-functionalized Carbon Quantum Dots for Chemical Sensing. *Carbon* **2012**, *50*, 2810−2815.

(21) Zhang, M.; Zhang, X. H.; He, X. W.; Chen, L. X.; Zhang, Y. K. A Self-Assembled Polydopamine Film on the Surface of Magnetic Nanoparticles for Specific Capture of Protein. *Nanoscale* **2012**, *4*, 3141−3147.

(22) Xue, C.; Han, Q.; Wang, Y.; Wu, J. H.; Wen, T. T.; Wang, R. Y.; Hong, J. L.; Zhou, X. M.; Jiang, H. J. Amperometric Detection of Dopamine in Human Serum by Electrochemical Sensor based on Gold Nanoparticles doped Molecularly Imprinted Polymers. *Biosens. Bioelectron.* **2013**, *49*, 199−203.

(23) Mao, Y.; Bao, Y.; Han, D. X.; Li, F. H.; Liu, L. Efficient One-pot Synthesis of Molecularly Imprinted Silica Nanospheres embedded Carbon Dots for Fluorescent Dopamine Optosensing. *Biosens. Bioelectron.* **2012**, *38*, 55−60.

(24) Cai, Z. J.; Shi, X. J.; Fan, Y. N.; Xiao, J.; Wang, S.; Liu, Y. Electrochemical Properties of Electrospun Polyindole Nanofibers as a Polymer Electrode for Lithium ion Secondary Battery. *J. Power Sources* **2013**, *227*, 53−59.

(25) Qian, T.; Wu, S. J.; Shen, J. Facilely Prepared Polypyrrole-reduced Graphite Oxide Core−Shell Microspheres with High Dispersibility for Electrochemical Detection of Dopamine. *Chem. Commun.* **2013**, *49*, 4610−4612.

(26) Qian, T.; Yu, C. F.; Zhou, X.; Ma, P. P.; Wu, S. S.; Xu, L. N.; Shen, J. Ultrasensitive Dopamine Sensor based on Novel Molecularly Imprinted Polypyrrole Coated Carbon Nanotubes. *Biosens. Bioelectron.* **2014**, *58*, 237−241.

(27) Routh, P.; Das, S.; Shit, A.; Bairi, P.; Das, P.; Nandi, A. K. Graphene Quantum Dots from a Facile Sono-Fenton Reaction and Its Hybrid with a Polythiophene Graft Copolymer toward Photovoltaic Application. *ACS Appl. Mater. Interfaces* **2013**, *5*, 12672−12680.

(28) Zhou, X.; Ma, P. P.; Wang, A. Q.; Yu, C. F.; Qian, T.; Wu, S. S.; Shen, J. Dopamine Fluorescent Sensors based on Polypyrrole/Graphene Quantum Dots Core/Shell Hybrids. *Biosens. Bioelectron.* **2015**, *64*, 404−410.

(29) Prasad, B. B.; Jauhari, D.; Tiwari, M. P. A Dual-template Imprinted Polymer-modified Carbon Ceramic Electrode for Ultra Trace Simultaneous Analysis of Ascorbic Acid and Dopamine. *Biosens. Bioelectron.* **2013**, *50*, 19−27.

(30) Qu, Z. B.; Zhou, X. G.; Gu, L.; Lan, R. M.; Sun, D. D.; Yu, D. J.; Shi, G. Y. Boronic Acid Functionalized Graphene Quantum Dots as a

Fluorescent Probe for Selective and Sensitive Glucose Determination in Microdialysate. *Chem. Commun.* **2013**, *49*, 9830−9832.

DOI: 10.1021/am5078478
ACS Appl. Mater. Interfaces 2015, 7, 11741−11747